JOURNAL OF VIROLOGY, Jan. 2003, p. 1195–1203 Vol. 77, No. 2
0022-538X/03/$08.00+0 DOI: 10.1128/JVI.77.2.1195–1203.2003

Two Distinct Mechanisms Ensure Transcriptional Polarity in Double-Stranded RNA Bacteriophages

Hongyan Yang, Eugene V. Makeyev, Sarah J. Butcher, Aušra Gaidelytė, and Dennis H. Bamford*

Department of Biosciences and Institute of Biotechnology, FIN-00014 University of Helsinki, Finland

Received 13 May 2002/Accepted 8 October 2002

In most double-stranded RNA (dsRNA) viruses, RNA transcription occurs inside a polymerase (Pol) complex particle, which contains an RNA-dependent RNA Pol subunit as a minor component. Only plus- but not minus-sense copies of genomic segments are produced during this reaction. In the case of ϕ6, a dsRNA bacteriophage from the *Cystoviridae* family, isolated Pol synthesizes predominantly plus strands using virus-specific dsRNAs in vitro, thus suggesting that Pol template preferences determine the transcriptional polarity. Here, we dissect transcription reactions catalyzed by Pol complexes and Pol subunits of two other cystoviruses, ϕ8 and ϕ13. While both Pol complexes synthesize exclusively plus strands over a wide range of conditions, isolated Pol subunits can be stimulated by Mn^{2+} to produce minus-sense copies on ϕ13 dsRNA templates. Importantly, all three Pol subunits become more prone to the native-like plus-strand synthesis when the dsRNA templates (including ϕ13 dsRNA) are activated by denaturation before the reaction. Based on these and earlier observations, we propose a model of transcriptional polarity in *Cystoviridae* controlled on two independent levels: Pol affinity to plus-strand initiation sites and accessibility of these sites to the Pol in a single-stranded form.

Double-stranded RNA (dsRNA) viruses infect organisms from prokaryotes to higher eukaryotes, with some of these viruses causing diseases in humans and economically important animals and plants (7). Despite substantial variations in their structural organization and host specificity, most dsRNA viruses share a common RNA metabolism scheme.

Upon cell entry, virions are converted into transcriptionally active core particles, which produce single-stranded RNAs (ssRNAs) of positive polarity using genomic dsRNAs as templates. The plus-sense ssRNAs are extruded into the cytoplasm and translated by the cellular protein synthesis machinery. The same ssRNA transcripts can also act as templates for the synthesis of complementary minus-sense strands (replication). Replication occurs inside the newly assembled core particles and is catalyzed by the viral polymerase (Pol). The minus-strand RNA remains associated with the plus-strand template, thus reconstituting the genomic dsRNA. Particles bearing the dsRNA can either support additional rounds of transcription or, alternatively, mature into virions. Both transcription and replication in dsRNA viruses thus depend on the virus-encoded Pol and occur in the interior of a large Pol complex particle. Because dsRNA, in principle, can program both plus- and minus-strand synthesis, all dsRNA viruses need to utilize a control mechanism(s) ensuring selective synthesis of plus strands during transcription.

The dsRNA bacteriophage ϕ6 and a group of related bacteriophages belong to the *Cystoviridae* family. Due to extensive biochemical, genetic, and structural studies, ϕ6 has become one of the best-characterized dsRNA viruses (19, 20). The organization of the ϕ6 virion is outlined in Fig. 1A. The ϕ6 genome consists of three dsRNA segments of known sequence, small (S), medium (M), and large (L) (8, 18, 21). The Pol complex of ϕ6 consists of four protein species: P1, P2, P4, and P7. P1 forms the protein coat (2, 4), P4 is the RNA packaging NTPase (9, 13, 24), and P7 is believed to stabilize the packaged RNA inside the complex (11, 12). We have recently shown that protein P2 is the RNA-dependent RNA Pol subunit, which catalyzes both replication and transcription in vitro (16, 17). As in the case of particle-based transcription, the ϕ6Pol-directed transcription in vitro proceeds via a semiconservative (strand-displacing) mechanism. Furthermore, with ϕ6-specific dsRNA templates, ϕ6Pol produces mainly plus-sense RNA copies. These data suggest that the template specificity of the Pol subunit might be a reason for the asymmetric transcription observed in the ϕ6 Pol complex in vivo. Interestingly, ϕ6Pol can selectively recognize plus-strand initiation signals on both dsRNA and ssRNA templates, thus indicating that transcription initiation is likely to occur on terminally open dsRNA molecules (16). The recently solved atomic structures of ϕ6Pol, as well as its complexes with nucleotides or/and template, have provided molecular insights into the initiation mechanism and, to some extent, explain the template selectivity of the enzyme (3).

Other members of the *Cystoviridae*, bacteriophages ϕ7 to ϕ13, also have tripartite dsRNA genomes (22). Of these, genomes of ϕ8 and ϕ13 have been sequenced completely (10, 26). Based on sequence comparisons, ϕ6 and ϕ13 are closer to each other than to ϕ8. So far, the RNA metabolism of ϕ8 and ϕ13 has not been studied in detail. An in vitro transcription system based on ϕ8 subviral particles (cores) has been described previously, but the polarity of the transcripts has not been determined (10). For ϕ13, no particle-based transcription system has been available.

We have recently purified Pol subunits (P2 proteins) from ϕ8 and ϕ13 and shown their RNA-dependent RNA polymer-

* Corresponding author. Mailing address: Department of Biosciences and Institute of Biotechnology, P.O. Box 56, Viikinkaari 5, FIN-00014 University of Helsinki, Finland. Phone: (358) 9 191 59100. Fax: (358) 9 191 59098. E-mail: dennis.bamford@helsinki.fi.

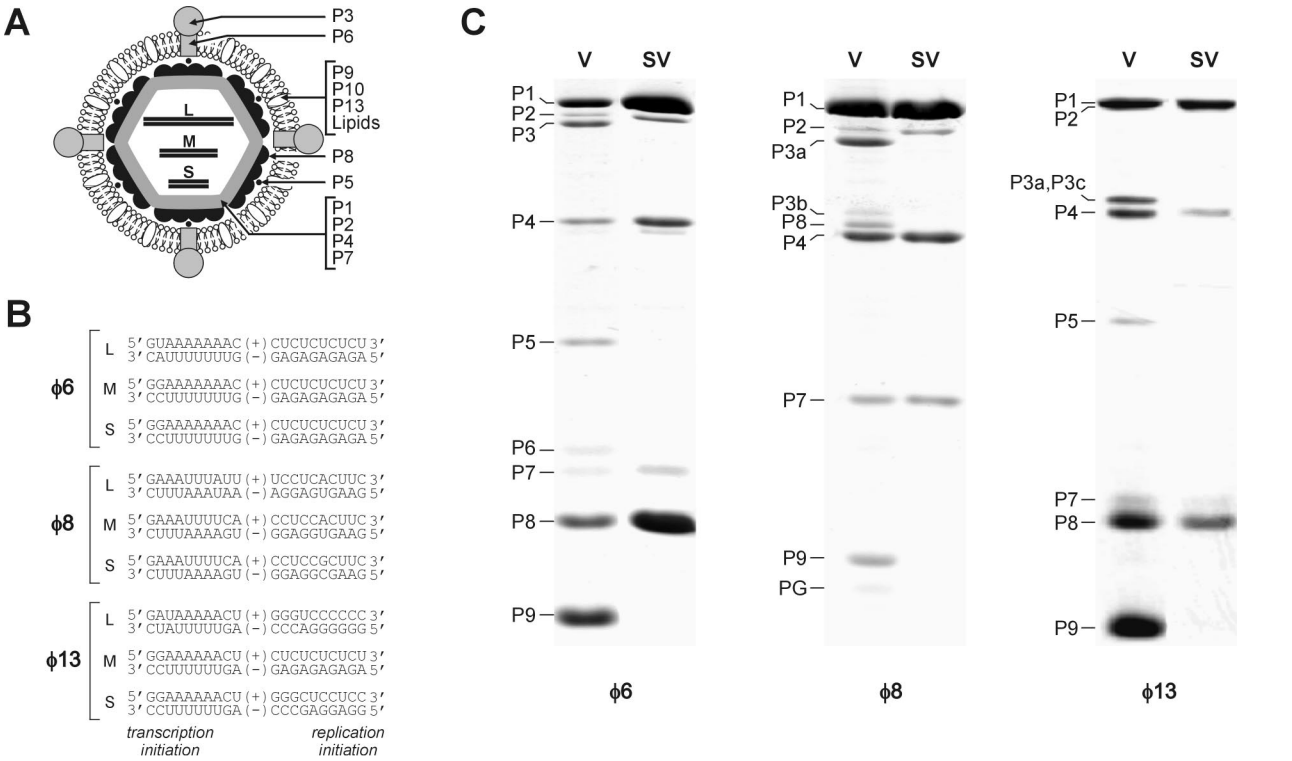

FIG. 1. Structural and genetic organization of *Cystoviridae*. (A) Diagram of ϕ6 virion. Proteins P1, P2, P4, and P7 form the virion core, which occludes three dsRNA segments, L, M, and S. The core is covered by the protein P8 shell. This P8-coated particle is called the NC. The NC is surrounded with the lipid-containing envelope, which also includes proteins P9, P10, and P13. Membrane-associated proteins P6 and P3 form the viral receptor-binding complex. Protein P5 is an endopeptidase residing between the P8 shell and the membrane. (B) Terminal sequences of genomic segments L, M, and S of bacteriophages ϕ6, ϕ8, and ϕ13. Positions of transcription and replication initiation sites are indicated. (C) Protein composition of virions (V) and subviral particles (SV) of ϕ6, ϕ8, and ϕ13. The proteins were separated by SDS–16% PAGE and stained with Coomassie blue G-250. ϕ6 NCs and ϕ8 cores were produced by Triton X-114 extraction. ϕ13 NCs were obtained by Triton X-100 extraction. Note that membrane proteins are underrepresented in the ϕ8 virion preparation due to particle instability.

ization activity in vitro (29). Like their ϕ6 counterpart, ϕ8Pol and ϕ13Pol can utilize both ssRNA and dsRNA templates, showing distinct template specificity profiles. The template preferences of the enzymes correlate partially with the terminal sequences of the ϕ8 and ϕ13 genomic segments. Notably, short sequences from minus-strand 3′ termini (transcription initiation sites) of phage-specific RNA segments have been shown to stimulate Pol-directed synthesis on chimeric ssRNA templates in vitro. However, a comparable stimulatory effect has been also observed for ϕ13Pol when RNA templates were extended with C-rich 3′-terminal sequences, like that from the 3′ end of the ϕ13 s^+ strand. Therefore, ϕ13Pol template specificity cannot be the sole reason for preferential plus-strand synthesis during in vivo transcription. It is also difficult to imagine how the ϕ8Pol subunit would discriminate between the plus- and minus-sense initiation sites in vivo, since all three segments are flanked with three-nucleotide inverted repeats (Fig. 1B).

To better understand transcriptional regulation in the *Cystoviridae*, we isolated subviral particles from ϕ8 and ϕ13 and assayed their transcriptional activity in vitro using strand-separating gel electrophoresis. Together with our earlier data, the results of this study suggest that transcription in the *Cystoviridae* is regulated by the interplay of two distinct mechanisms: (i) Pol template preference for plus-sense initiation sites and (ii) higher accessibility of transcription initiation sites in an initiation-competent single-stranded form. This study also supports the long-standing hypothesis that genomic segments of dsRNA viruses might be partially unwound in the interior of the Pol complex.

MATERIALS AND METHODS

Isolation of nucleocapsids (NCs). Virions of ϕ13 and ϕ8 were purified as described previously (10, 26) with some modifications. *Pseudomonas syringae* LM2489 was chosen as the host for both ϕ13 and ϕ8. To produce pure virions of ϕ13, the host cells were grown to a density of 1.5×10^8 CFU/ml in LB-broth at 28°C and then transferred to 23°C and grown to a density of 2×10^8 CFU/ml. ϕ13 was added at a multiplicity of infection of 10 to 15, and the culture was grown until lysis occurred. After removal of cell debris by centrifugation at 8,000 rpm (Sorvall SLA 3000 rotor) for 10 min at 4°C, virions were concentrated with 10% (wt/vol) polyethylene glycol (PEG) 6000–0.5 M NaCl and purified on 5-to-20% (wt/vol) sucrose gradients in 50 mM sodium phosphate, pH 7.0 (centrifuged at 24,000 rpm for 1 h at 15°C; Sorvall AH629 rotor). The light-scattering zones containing viruses were collected, pelleted at 32,000 rpm (Sorvall T647.5 rotor) for 2 h 30 min at 4°C, and resuspended in 50 mM $NaHPO_4$, pH 7.0, on ice. To obtain pure ϕ8 virions, the host cells were grown to a density of 10^8 CFU/ml in a modified LB-broth (Luria-Bertani broth containing 2 mM $MgCl_2$ and 1% NaCl) at 28°C and then transferred to 23°C and infected at a density of 1.5×10^8 CFU/ml (multiplicity of infection = 30). Incubation was continued until lysis occurred. The virions of ϕ8 were further purified as described above and resuspended in ice-cold buffer containing 10 mM $KHPO_4$, 1 mM $MgCl_2$, and 200 mM NaCl, pH 7.5 (buffer A).

ϕ8 cores were isolated similarly to ϕ6 NC by phase separation with Triton

X-114 (1). The only difference was that ϕ8 virions were not treated with butylated hydroxytoluene. The isolated subviral particles were pelleted through a 20% (wt/vol) sucrose cushion in buffer A and resuspended in ice-cold buffer A. ϕ13 NC was isolated with Triton X-100 as described previously for ϕ6 NC (6) with some modification. Briefly, purified virions were diluted to ~1 mg/ml with buffer A, and Triton X-100 was added to 2%. The mixture was incubated for 5 min at room temperature and layered onto the top of a 20% sucrose cushion containing buffer A and 0.1% Triton X-100. The samples were pelleted at 40,000 rpm (rotor T865; Sorvall) at 10°C for 3 h. The pellet was rinsed three times with buffer A and then dissolved overnight in ice-cold buffer A containing 0.1% Triton X-100. The protein concentration was determined using the Bradford assay. The subviral particles were either used immediately for transcription reactions in vitro or stored in aliquots at −80°C for later use. The protein composition of the virions and subviral particles was analyzed by sodium dodecyl sulfate–16% polyacrylamide gel electrophoresis (SDS–16% PAGE).

CryoEM. For cryo-electron microscopy (CryoEM), aliquots of the sucrose band containing virions or ϕ6 or ϕ8 cores were concentrated by rapid pelleting (29 lb/in^2 in a Beckman Airfuge, A95 rotor, at 15°C for 8 min). The pellet was rinsed and resuspended in the appropriate buffer (ϕ6 virus, 20 mM Tris [pH 7.4]; ϕ6 cores, 20 mM Tris [pH 8], 50 mM NaCl; ϕ8 virus, potassium phosphate [pH 7.5], 20 mM NaCl, 1 mM $MgCl_2$; ϕ8 cores, 10 mM potassium phosphate [pH 7.5], 1 mM ATP, 20 mM NaCl, 1 mM $MgCl_2$, ϕ13 virus, 10 mM potassium phosphate [pH 7.2]) to approximately 1 mg/ml. To prepare ϕ13 NC, 350 μl of purified virus (0.5 mg/ml) in buffer B (10 mM sodium phosphate [pH 7.0], 1 mM ATP, 150 mM NaCl) was treated with 0.1% Triton X-100 for 5 min at room temperature and pelleted through a 100-μl 20% sucrose cushion in buffer B (29 lb/in^2 in a Beckman Airfuge, A95 rotor, at 15°C for 12 min). The pellet was rinsed and resuspended in 40 μl of buffer B. Samples were immediately vitrified (5) onto holey carbon-coated grids (Quantifoil microtools Ltd, Jena, Germany) in liquid ethane and transferred to either a Gatan 626 or an Oxford CT3500 cryostage for observation in either a Philips Tecnai 12 biotwin microscope operating at 120 kV or a Philips Tecnai F20 FEG microscope operating at 200 kV. Micrographs were recorded on Kodak SO-163 film under low-dose conditions (5).

Particle-based transcription in vitro. The protein concentration of the subviral particle preparations was adjusted to 0.3 mg/ml with 20 mM Tris-HCl (pH 8.0)–100 mM NaCl–1 mM ATP for ϕ6 and with 10 mM KH_2PO_4–1 mM $MgCl_2$–200 mM NaCl (pH 7.5) for ϕ8 and ϕ13. Transcription reactions were typically carried out at 37°C for 1 h, in 33-μl mixtures containing 10 μl of diluted ϕ6 or ϕ13 NCs or ϕ8 cores, 16 μl of 2× transcription reaction mixture, 3 μl of 50% PEG 6000, 1 μl of RNasin (40 U/μl; Promega) and 2 μCi of [α-^{32}P]UTP (~3,000 Ci/mmol; catalog no. PB10203; Amersham Biosciences). The 2× transcription reaction mixture contained 100 mM Tris-HCl, pH 8.9; 200 mM KCl; 100 mM NH_4Cl; 3 to 6 mM $MnCl_2$ (3 mM for ϕ6 and ϕ8; 6 mM for ϕ13); 10 mM dithiothreitol; a 2 mM concentration (each) of ATP, CTP, and GTP; and 0.2 mM UTP. The reactions were terminated by adding 3.5 μl of 10% SDS, and the products were purified using Sephadex G-50 spin columns (Amersham Biosciences) equilibrated with water and analyzed by strand-separating gel electrophoresis.

Strand-separating agarose gel electrophoresis. Strand-separating electrophoresis was carried out in 1% agarose gels buffered with TBE (50 mM Tris-borate, 1 mM EDTA, pH 8.3) without ethidium bromide (EtBr) as described previously (25). To prepare denatured samples, RNA was dissolved in loading buffer U2 (8 M urea, 10 mM EDTA, 0.2% SDS, 6% [vol/vol] glycerol, 0.05% bromophenol blue, and 0.05% xylene cyanol), boiled for 4 min, cooled on wet ice for 4 min, and immediately run into the gel to prevent reannealing. In the case of particle-based transcription, RNA samples were prepared by treating ϕ6 and ϕ13 NCs or ϕ8 cores with 1% SDS for 10 min at room temperature followed by phenol-chloroform extraction. The aqueous phase was passed through Sephadex G-50 spin columns, denatured, and subjected to gel analysis. Electrophoresis was carried out for 7.5 to 8 h at ~5 V/cm and room temperature. The gels were stained with EtBr (0.5 μg/ml) and photographed. For autoradiography, gels were dried and exposed with Fuji Super RX film or analyzed with a Fuji BAS1500 phosphorimager.

Oligonucleotide probes. Oligonucleotide probes were prepared by labeling the synthetic oligonucleotides listed in Table 1 with [γ-^{32}P]ATP using T4 polynucleotide kinase as described elsewhere (27). Briefly, 20-μl reaction mixtures contained 10 pmol of an appropriate oligonucleotide, 10 pmol of [γ-^{32}P]ATP (~3,000 Ci/mMol; catalog no. AA0068; Amersham Biosciences), and 10 U of T4 polynucleotide kinase (Fermentas) in the reaction buffer provided by the manufacturer. Reactions were incubated at 37°C for 1 h and then purified through Sephadex G-50 spin columns equilibrated with water.

Northern blot analysis. RNAs separated by 1% TBE (pH 8.3) strand-separating gels were partially hydrolyzed, neutralized, and transferred to nylon membranes (GeneScreenPlus; NEN) as described elsewhere (25). After the transfer, the membranes were preincubated in a hybridization solution (ExpressHyb; Clontech) for 1 h at 40°C, which was followed by overnight hybridization under the same conditions with labeled probes (~10^5 cpm/ml) prepared as described above. After hybridization, the filters were successively washed with 2× SSC (1× SSC is 0.15 M NaCl plus 0.015 M sodium citrate)–0.05% SDS and 0.1× SSC–0.1% SDS, air dried, and exposed to Fuji Super RX film or analyzed with a Fuji BAS1500 phosphorimager.

TABLE 1. Oligonucleotides used in this study

Oligonucleotide[a]	Sequence (5′ to 3′)
phi8S	GATAAAGCATATGGGTAGAATCTTTCAACTGT
phi8M	GAGCTTCATATGCTGATTAAGAACCTG
phi8L	CGAGCCGTACATATGGCATCGTTCGT
phi13S	ACGAGTGCGAAACGTATAAGGATATATGACATGGGTCTGT
phi13M	AACTGACTGAGATTCTTTCGGTTTCTGAGTTCGACGGTAC
phi13L	CAGGCGCTGACATATGACTTCCCGCT
anti-phi8S	GCGAATTCAGCATCACGAACGCTTCTCCTT
anti-phi8M	AGTAAGCTTATCATACGGCCACCGGAA
anti-phi8L	GGAGTTGGATCCTGGTGTAACTTTCGT
anti-phi13S	ACAGACCCATGTCATATATCCTTATACGTTTCGCACTCGT
anti-phi13M	TGACCGTCGAACTCAGAAACCGAAAGAATCTCAGTCAGTT
anti-phi13L	GCCGAAGCTTATCTGACATCCCTCGT
phi6M_term_up	GGGGGCTCTCTCTCTAGGTCTTCG
phi6M_term_down	AATTCGAAGACCTAGAGAGAGAGCCCCCTGCA

[a] Oligonucleotides beginning with the prefix "anti-" are complementary to the plus-sense strands.

In vitro transcription with purified Pol subunits. RNA substrates were prepared as described earlier (29). Plasmid pHY3 encoding $m^+\Delta T$ RNA was derived from pLM656 (23) by substituting its small *Pst*I-*Eco*RI fragment with the duplex of oligonucleotides phi6M_term_up and phi6M_term_down (Table 1). In vitro RNA synthesis with Pol subunits was carried out as described in reference 29 with some modifications. The mixtures typically contained 25 mM HEPES-KOH (pH 7.4 for ϕ13Pol; pH 7.8 for ϕ6Pol) or 25 mM Tris-HCl, pH 9.3, for ϕ8Pol; 10 mM ammonium acetate (NH_4OAC); 3% (wt/vol) PEG 4000; 2.5 mM $MgCl_2$; 0 to 10 mM $MnCl_2$ (see Results for details); 0.05 mM EDTA; 0.05% Triton X-100; a 0.5 mM concentration (each) of ATP and GTP; a 0.1 mM concentration (each) of CTP and UTP; RNasin, 0.4 U/μl; and [α-^{32}P]UTP, 0.25 mCi/ml. The final concentration of RNA substrates was 25 to 100 μg/ml. Reactions were initiated by adding one of the three Pol subunits up to 0.01 mg/ml and further incubated at 30°C for 1 h. Reaction products were purified with Sephadex G-50 spin columns and subjected to strand-separation electrophoresis as described above.

RESULTS

Preparation of ϕ8 and ϕ13 subviral particles. The virion of ϕ6 can be subdivided into three major structural elements: (i) inner core containing genomic RNA, (ii) P8 protein shell surrounding the core, and (iii) a phospholipid envelope containing membrane-associated proteins (Fig. 1A). Subviral particles containing both the core and the P8 shell are called NCs. In the case of ϕ6 and ϕ8, it has been possible to isolate transcriptionally active subviral particles by removing the envelope with nonionic detergents (1, 10). Similarly, we used here extraction with Triton X-100 to obtain transcriptionally active particles of ϕ13. As judged by SDS-PAGE analysis, subviral particles produced in this manner for all three bacteriophages are essentially free of the membrane-associated proteins (Fig. 1C). In ϕ6 and ϕ13, P8 protein remains associated with the viral cores (NCs), whereas in the case of ϕ8 this protein is removed

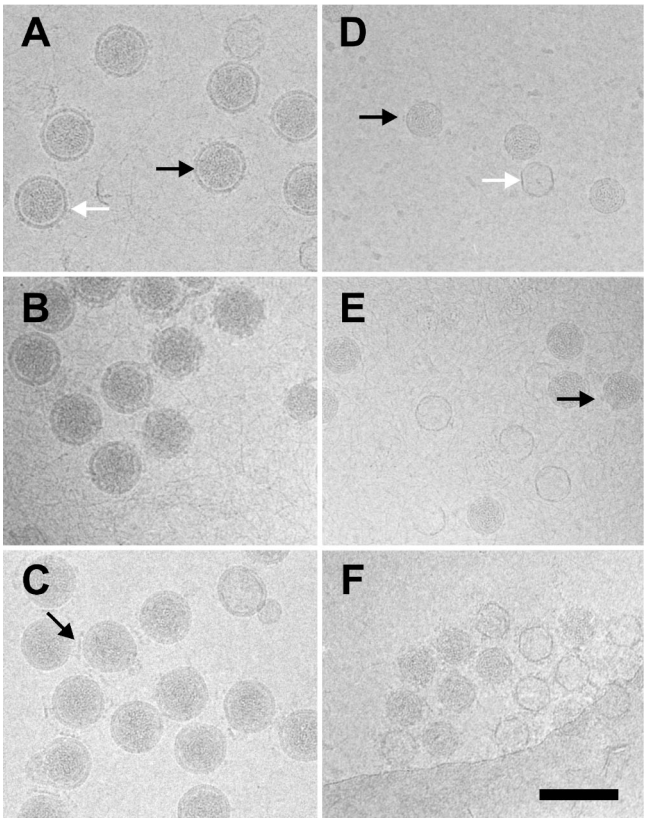

FIG. 2. CryoEM of *Cystoviridae*. The morphologies of the ~85-nm-diameter virions of ϕ6 (A), ϕ8 (B), and ϕ13 (C) are very similar. ϕ6 (D) and ϕ8 (E) cores appear as ~50-nm-diameter particles; (F) ϕ13 NCs are ~58-nm-diameter particles. (A) The virion membrane is clearly visible (black arrow) as are the spikes (white arrow). (C) There is often intervirus intercalation of ϕ13 virion spikes seen as straight lines about 35 nm long between virions (black arrow), perhaps mediated by the presence of phospholipid. (D and E)The ϕ6 cores have 12 turrets projecting from the surface that are also visible in ϕ8 cores (black arrows). Cores that have lost their RNA are seen in all preparations as closed circles (white arrow in panel D). The scale bar represents 100 nm in all panels.

together with the membrane (cores) (Fig. 1C), in accordance with a previous observation (10). We also prepared ϕ6 cores as described previously (1) and used those for CryoEM.

To ensure the integrity of the particles used, virions, NCs, and cores were examined by CryoEM. Virions from all three viruses were similar in appearance and size, with a diameter of ~85 nm (Fig. 2) (14). In all three cases, the spike-containing membrane is clearly seen surrounding the RNA-filled NCs. Interestingly, ϕ13 consistently contained the highest complement of spikes (Fig. 2C). Virion preparations of ϕ8 already contained ~80% cores even before the detergent treatment, explaining the low specific infectivity of this virus. Isolated ϕ8 cores were similar in appearance to ϕ6 cores (~50 nm in diameter), including ~4-nm protrusions at the vertices corresponding to the packaging protein P4 (2, 4). When the RNA is lost from the particles, only an empty shell remains (Fig. 2D). ϕ13 NCs have an extra layer of protein P8 on the outside, giving them a rough appearance compared to ϕ6 and ϕ8 cores, and a larger diameter (~58 nm), similar to that of ϕ6 NCs. The ϕ6 and ϕ13 NCs and ϕ8 core preparations were used in the subsequent in vitro transcription experiments.

Strand-separating gel electrophoresis of ϕ8 and ϕ13 RNAs. As a tool for determining the polarity of newly synthesized RNA strands, we adapted a strand-separating gel electrophoresis protocol by Pagratis et al. (25) for the ϕ8 and ϕ13 genomic RNAs. The RNAs were denatured by heat and then analyzed using TBE agarose gel electrophoresis as specified under Materials and Methods. RNA bands were visualized with EtBr staining or/and autoradiography. For both ϕ8 and ϕ13, six distinct bands could be discerned in the gel, thus indicating that all plus and minus strands were separated (Fig. 3A). Only five bands were present in the ϕ6 control, including individual plus- (s^+ and m^+) and minus-sense (s^- and m^-) strands and an unresolved l^+/l^- band, as expected (25). To identify individual RNA bands of ϕ8 and ϕ13, gel-separated products were transferred to a nitrocellulose membrane and probed with labeled, strand-specific oligonucleotides. As a result, all of the ϕ8 and ϕ13 RNA bands were unambiguously identified as either plus or minus strands of L, M, or S segments (Fig. 3B and C). Curiously, plus strands always migrated faster than corresponding minus strands. Since the two complementary strands are of the same length, the higher mobility of the plus RNA species apparently indicates their more compact shape. One possible rationalization of this fact is that plus-sense transcripts occur in vivo in a ssRNA form and have to withstand cellular nucleases, while minus strands are only found inside viral cores as a part of dsRNA genome segments.

Subviral particles of ϕ8 and ϕ13 synthesize plus strands. To analyze the products of ϕ8 and ϕ13 particle-based reactions, ϕ8 cores and ϕ13 NCs were incubated for 1 h at 28°C in a buffer containing all four nucleoside triphosphates and divalent metal ions, after which RNA was extracted and analyzed by strand-separating gel electrophoresis. A ϕ6 NC transcription reaction was also set up as a positive control. Both ϕ8 and ϕ13 particles synthesize RNA in vitro, plus strands being the major reaction products (Fig. 4). The l^+ segment was underrepresented in the case of the ϕ6 and ϕ13 NC reactions. On the contrary, ϕ8 cores produced nearly equimolar amounts of all three plus strands, in line with an earlier finding (10). This difference in the product distribution is expected, as the plus-strand initiation sites are similar in all three ϕ8 segments, while being distinct between L and the other two segments of ϕ6 and ϕ13 (Fig. 1B).

Transcription in vitro catalyzed by purified Pol subunits. We then turned to another type of in vitro transcription system based on isolated Pol subunits and dsRNAs extracted from the virions (for brevity, we refer to this as the Pol/dsRNA system). Although Pol-catalyzed transcription has been reported recently for ϕ8 and ϕ13 (29), it has not been characterized in much detail. While optimizing the reaction conditions we observed that, in the presence of a fixed Mg^{2+} concentration, Mn^{2+} stimulated the ϕ6 Pol/dsRNA transcription maximally at 3 mM and stimulated the ϕ8 Pol/dsRNA transcription maximally at 1 mM (Fig. 5A and B). Higher Mn^{2+} concentrations inhibited ϕ8Pol activity sharply (Fig. 5B), which is consistent with our previous data on the Mn^{2+} dependence of the ϕ8Pol directed replication of ssRNA (29). Changes in Mn^{2+} concentration also affected transcription in the ϕ13 Pol/dsRNA system, but in a more complex manner. The optimum concentra-

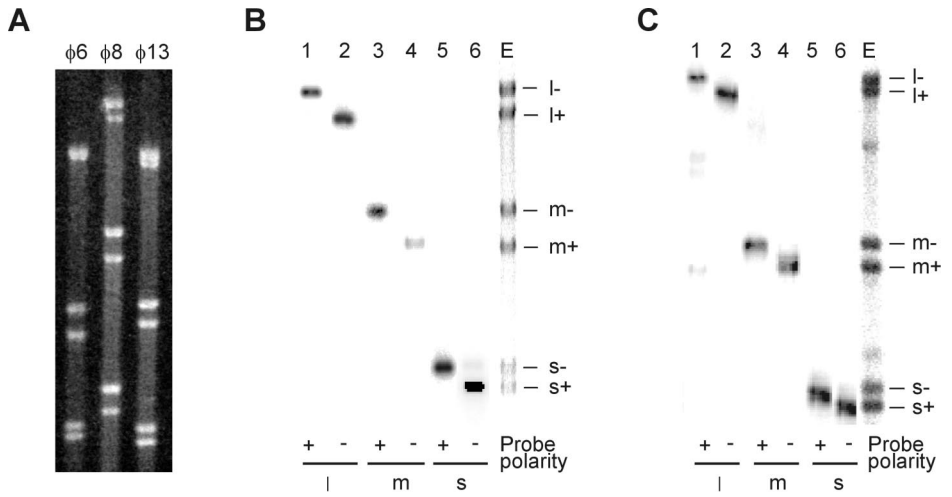

FIG. 3. Strand-separating gel electrophoresis of individual RNA strands from ϕ6, ϕ8, and ϕ13. (A) EtBr staining. (B) Northern blot analysis of ϕ8 RNAs. Lanes 1 to 6, gel-separated RNAs were transferred to nitrocellulose membrane and hybridized with strand-specific probes indicated below. Lane E contains heat-denatured ϕ8 RNA stained with EtBr. (C) Same analysis performed for ϕ13 RNAs. Strand assignment is shown on the right of the panels. I^+, m^+, and s^+ indicate the plus strands, and I^-, m^-, and s^- are the minus strands.

tion for L segment transcription was ~1 mM, whereas S and M were labeled with the highest intensity at ~5 mM (Fig. 5C). As a result, transcriptional activity of the three segments is nearly equal at 0.5 to 1 mM Mn^{2+}, shifting to predominant utilization of the S segment with increasing manganese concentration. Interestingly, manganese dependence of the particle-based transcription was generally similar to that of the relevant Pol/dsRNA systems (Fig. 5D to F). However, one substantial difference was that ϕ13 NCs tolerated elevated Mn^{2+} concentrations better than the corresponding Pol/dsRNA system (Fig. 5C and F).

Strand polarity in Pol-directed transcription. In the next experiment, the strand polarity of the Pol-directed transcription products was determined by strand-separating electrophoresis (Fig. 6). For the ϕ6 and ϕ8 Pol/dsRNA systems, newly produced plus strands were clearly more abundant than the corresponding minus strands. This distribution remained virtually unchanged over a range of reaction conditions including variations in Mn^{2+} concentration (not shown). Notably, the correct distribution of transcription products (more plus strands) was also observed for reaction mixtures containing ϕ6 and ϕ8 dsRNAs and heterologous Pol subunits (Fig. 6A and B). In fact, ϕ13Pol transcribed ϕ8 segments more accurately than ϕ8Pol. In the case of ϕ13 Pol/dsRNA transcription, only plus strands were produced when Mn^{2+} was absent from the reaction mixture (Fig. 6E). However, with an increase in manganese concentration, the distribution of the reaction products for the small segment changed toward minus-strand synthesis. Nearly equimolar amounts of s^+ and s^- were synthesized at 0.5 to 1 mM Mn^{2+}, and further increases in Mn^{2+} concentration led to preferential s^- synthesis. A similar tendency was also found for ϕ6Pol/ϕ13 dsRNA and ϕ8Pol/ϕ13 dsRNA transcription systems (Fig. 6C and D). In general, the transcriptional specificity of all of the Pol/dsRNA transcription reactions was clearly less strict than that of the particle-based systems (compare with Fig. 4).

Thermal activation of dsRNA templates increases Pol initiation fidelity. It has been shown earlier that, in addition to intact ϕ6 dsRNA, ϕ6Pol selectively recognizes plus-strand initiation signals on thermally denatured ϕ6 dsRNAs (see Fig. 6 in reference 17). We therefore studied the template specificity of ϕ8Pol and ϕ13Pol on preheated dsRNA templates. For this purpose, RNAs were briefly incubated at 100°C, chilled on ice, and added to the transcription mixture. This treatment was sufficient to convert most of the dsRNA to an ssRNA form (not shown). Upon incubation at 30°C, reaction products were analyzed by strand-separating electrophoresis. Control reaction mixtures containing intact dsRNAs were also analyzed (Fig. 7). Consistent with our previous observation for ϕ6, boil-

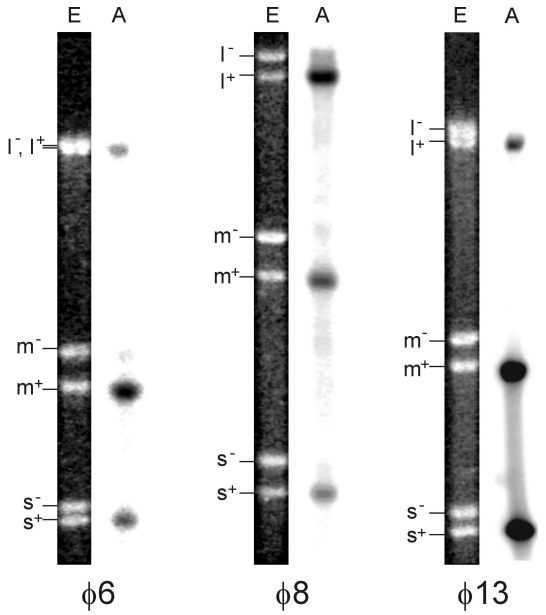

FIG. 4. Plus-sense RNA copies are produced in particle-based transcription in vitro. NC-core transcription was carried out as described in Materials and Methods, and total RNA was analyzed using strand-separating gel electrophoresis. Lanes E contain EtBr staining; lanes A are autoradiograms. Positions of the virus-specific strands are shown on the left.

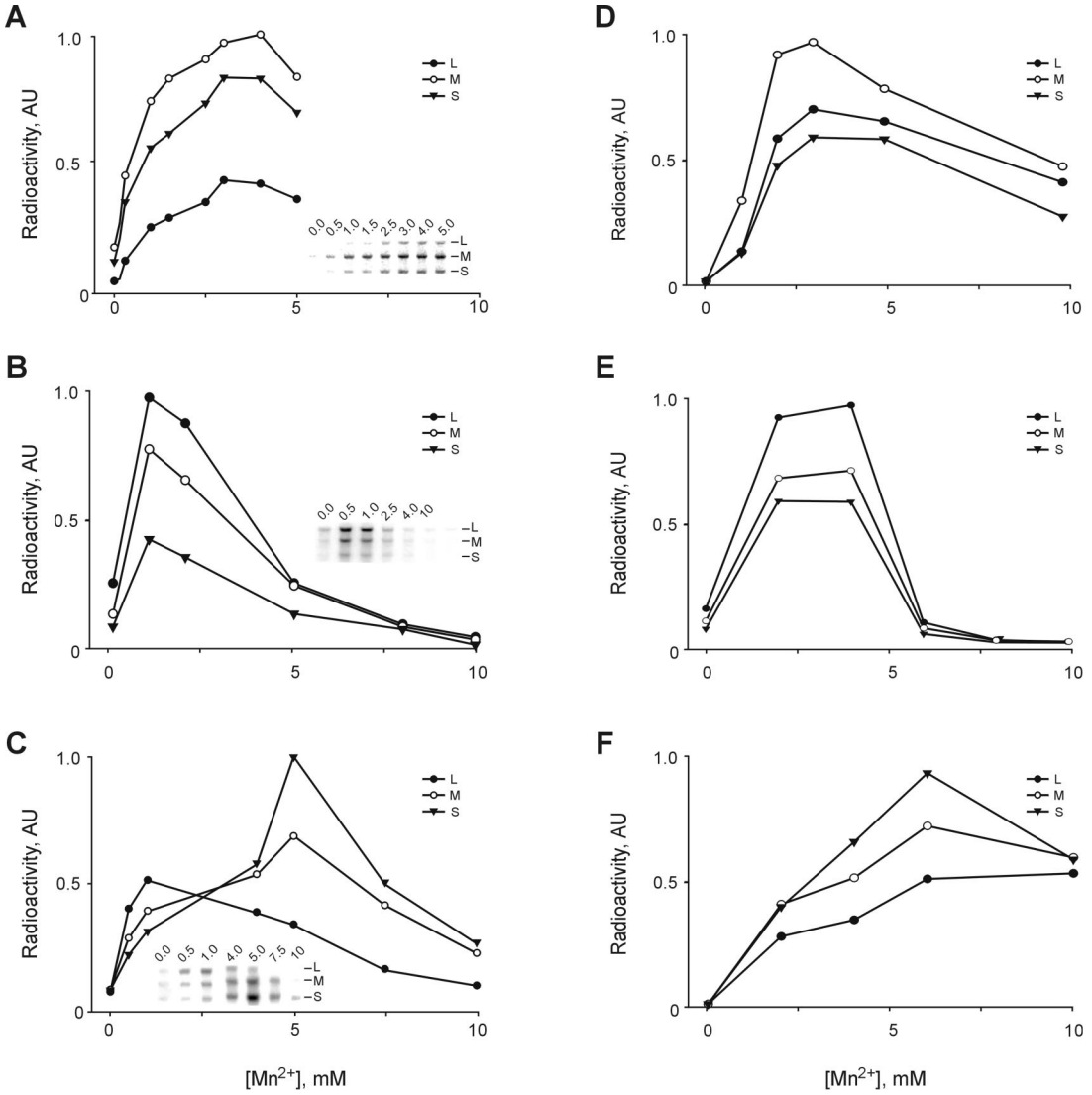

FIG. 5. Effect of Mn^{2+} concentration on the transcription activity of purified polymerase subunits and particle-based systems. (A) Reaction mixtures contained ϕ6Pol and ϕ6 dsRNA. (B) ϕ8Pol and ϕ8 dsRNA. (C) ϕ13Pol and ϕ13 dsRNA. Insets in panels A to C show autoradiograms of the original gels used for quantification. (D) Transcription by ϕ6 NCs. (E) ϕ8 cores. (F) ϕ13 NCs.

ing increased overall synthesis by approximately 1 order of magnitude for all three Pol/dsRNA systems. A less expected result was a significant increase in Pol initiation fidelity observed for all three transcription systems: plus strands constituted the overwhelming majority of the reaction products. Interestingly, ϕ13Pol produced only plus-sense copies of the small ϕ13 segment even in the presence of manganese ions. Overall, the distribution of the reaction products in the case of preheated RNAs was very similar to the patterns observed for the particle-based systems (Fig. 4).

Stable 3′-proximal secondary structure inhibits plus-strand template activity. One possible explanation for the increased fidelity in the case of heat-denatured dsRNA templates might be a stable secondary structure in the 3′-terminal region of plus-sense RNAs. Indeed, all three plus strands of all three viruses contain 3′-proximal sequences that are likely to fold into elaborate stem-loop elements (see references 10, 15, and 26 and references therein). Because the Pol subunit can only accommodate ssRNA in its template channel (3), these structures may interfere with efficient initiation. To test this hypothesis, a mutated ϕ6 m^+ segment was constructed that lacks the 3′-proximal cloverleaf-like secondary structure element while retaining the 15-nt wild-type 3′-terminal sequence ($m^+\Delta T$) (Fig. 8A). Template efficiency of this RNA in the ϕ6 Pol system was approximately 1 order of magnitude higher than that of the wild-type template, thus suggesting that secondary structure could indeed inhibit RNA synthesis initiation (Fig. 8B). A similar enhancement was observed when the 3′ of m^+ was replaced by a 3′ portion of s^- segment ($5'\Delta m^+_s$ RNA) (Fig. 8), as documented earlier (16).

DISCUSSION

In all dsRNA viruses, multiple copies of plus-sense RNA are transcribed within viral cores from genomic RNA segments and then used either as mRNAs or for the following rounds of

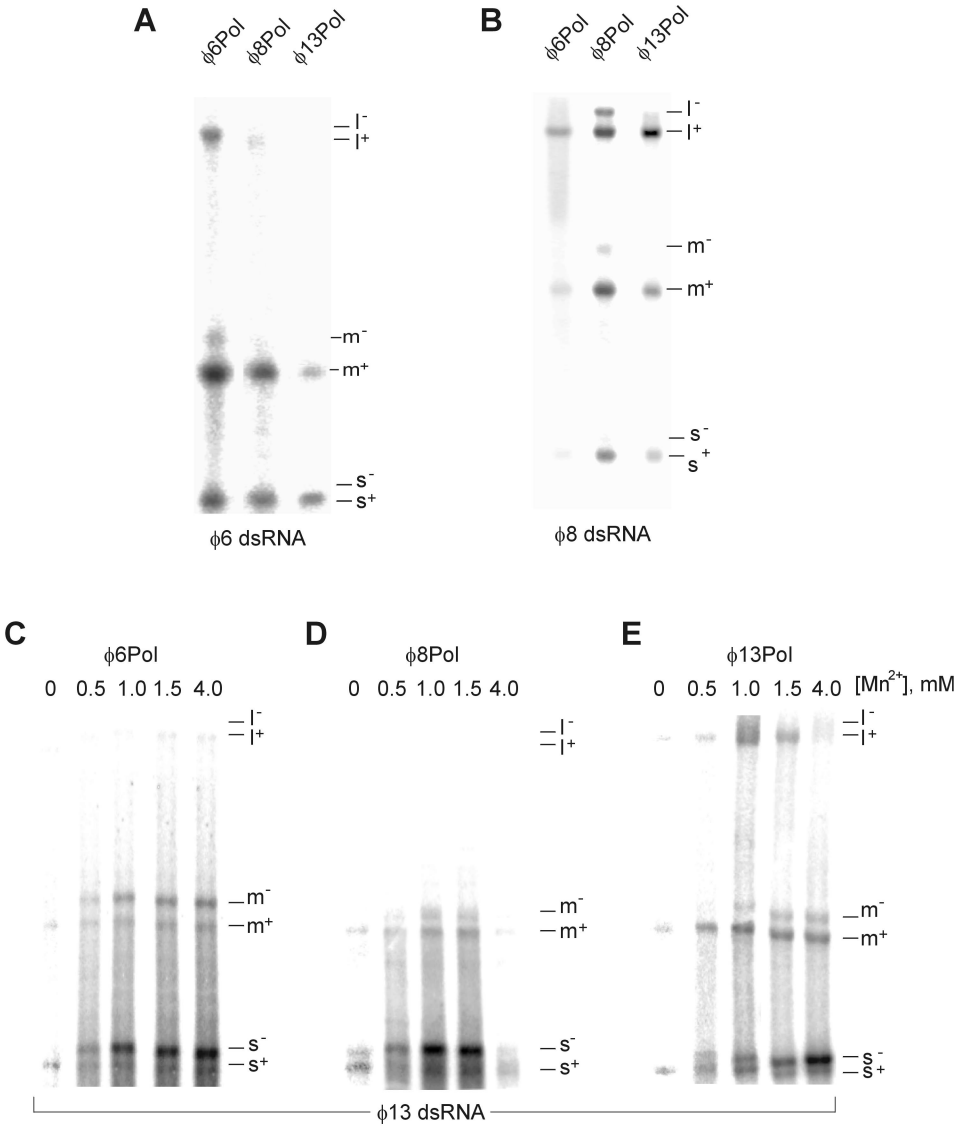

FIG. 6. Transcript polarity in different Pol/dsRNA systems dissected by strand-separating electrophoresis. Transcription on ϕ6 dsRNA (A) and ϕ8 dsRNA (B) templates catalyzed by purified ϕ6, ϕ8, or ϕ13 Pol subunit. The optimal Mn^{2+} concentration was used for each of the three enzymes: 3 mM for ϕ6Pol, 1 mM for ϕ8Pol, and 5 mM for ϕ13Pol. (C to E) Transcription on ϕ13 dsRNA template by the three Pol subunits at different concentrations of Mn^{2+}. Positions of the individual strands are shown on the right.

replication. The mechanisms of transcriptional regulation in dsRNA bacteriophages (*Cystoviridae*) have been studied previously using ϕ6 particle-based and Pol subunit-based transcription systems (1, 16, 22). One interesting observation was that purified ϕ6Pol produced plus-sense RNA products more efficiently than the minus-sense ones, on both ssRNA and dsRNA templates (16). This led us to conclude that transcriptional polarity in ϕ6 might be controlled by the Pol subunit via preferential initiation on short single-stranded stretches at the 3′ termini of minus strands (transcription initiation sites). In line with this model, structural data indicate that ϕ6Pol can only accommodate ssRNA but not dsRNA in its template-binding channel (3).

In a search for additional levels of regulation, we compared here particle- and Pol-based transcription reactions for ϕ6, ϕ8, and ϕ13. For this purpose, we optimized the production of ϕ13 NCs and ϕ8 cores for transcription in vitro. Comparison of these preparations by protein analysis and CryoEM revealed dsRNA-containing particles of the expected composition. Further, a strand-separating electrophoresis procedure was devised that allows one to separate all six RNA strands of both the ϕ8 and ϕ13 genomes. As expected, all three particle-based transcription systems yielded plus-sense RNA transcripts, with very little or no minus-strand products (Fig. 4). Similarly to the previous data on ϕ6 (16), the Pol/dsRNA systems retain a substantial degree of this transcriptional specificity: ϕ8Pol was clearly biased towards the plus-strand synthesis on phage-specific dsRNA templates over a range of reaction conditions (Fig. 5 and 6). ϕ13 Pol/dsRNA transcription also produced plus-sense products, but only when no Mn^{2+} was present in the reaction mixture. Increase in $[Mn^{2+}]$ dramatically stimulated production of minus-sense copies of the ϕ13 small segment

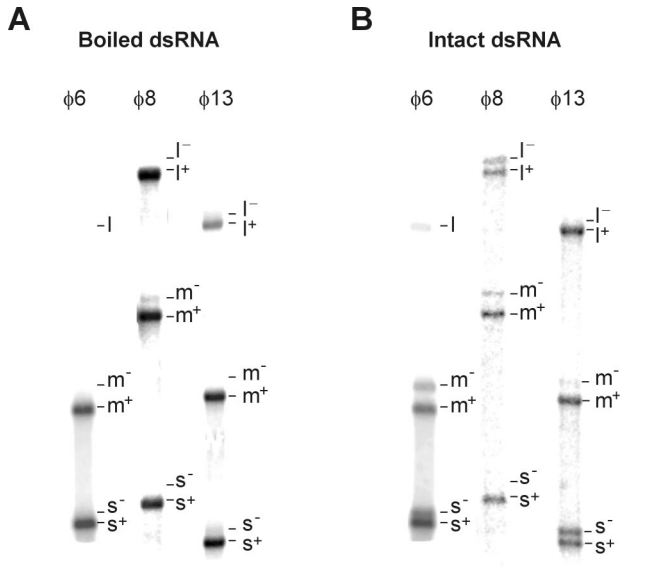

FIG. 7. Pol-directed transcription with denatured dsRNA templates. Transcription was performed as described in Materials and Methods using either heat-denatured (A) or intact (B) dsRNA samples and analyzed by strand-separating electrophoresis. Mn^{2+} concentration was 1 mM in all reaction mixtures. Positions of individual strands are shown on the right of each lane. Panel A is overexposed compared with panel B.

(Fig. 5C and 6E). This observation is in line with our previous results showing that the initiation efficiency of ϕ13Pol on ssRNA templates varies depending on the 3′-terminal sequence. Specifically, initiation was more efficient for templates that terminated with CC3′ (as in ϕ13 m^-, s^-, and s^+) than those that terminated with CU3′ (as in ϕ13 m^+) (for reference, see Fig. 1B). Thus, terminal preferences of ϕ13Pol might account for the preferential synthesis of the plus-sense copy of the M segment observed in this study (Fig. 6E). However, in the case of S segment, mechanisms other than Pol template preference obviously affect the plus- to minus-sense product ratio.

Several lines of evidence suggest that this mechanism might be related to the availability of RNA termini in an initiation-competent single-stranded form. Theoretically, the G+C content of the transcription initiation sites (Fig. 1B, left-hand termini) is lower than that of the replication initiation sites (Fig. 1B, right-hand termini). Therefore, transcription termini are less likely than replication termini to form stable duplexes. On the experimental side, the transcript pattern in heterologous Pol/dsRNA mixtures depended more on the origin of dsRNA than on the Pol source (Fig. 6). This is particularly true for ϕ8 dsRNA, whose plus-sense initiation signal is recognized by all three Pol subunits, despite well-documented differences in the template specificity profiles between ϕ8Pol on the one hand and ϕ6 and ϕ13 Pol subunits on the other (29). Conversely, ϕ8Pol faithfully transcribes ϕ6 dsRNA. It is sensible to suggest that heterologous (and, to some extent, homologous) Pol subunits utilize the more accessible rather than the most-efficient initiation sites. On the molecular level, accessibility can be realized as more intensive "fraying" of A+U-rich transcription initiation sites, replication termini being fastened by multiple G-C base pairs (Fig. 1B).

However, the transcription experiment with denatured dsRNA templates offers an alternative explanation (Fig. 7). Indeed, according to the fraying model, one would expect transcriptional polarity to disappear upon dsRNA denaturation for all three ϕ8 genomic segments and for ϕ13 S and L segments (Fig. 1). However, denaturation actually improves initiation fidelity to the level comparable with the NC-core-based systems. This indicates that intra- rather than intermolecular RNA secondary structure might provide a reason for the differing accessibility of the 3′ termini. This is consistent with the presence of conserved 3′-proximal secondary structure elements in plus strands of all three bacteriophages (see references 10, 15, and 26 and references therein). On the contrary, no stable secondary structure is predicted for the 3′ termini of minus strands. Our experiments with the modified ϕ6 m^+ segment that lacks the wild-type 3′ cloverleaf structure support this model (Fig. 8).

It is intriguing to hypothesize that the above mechanism might function in the context of the transcriptionally active, subviral particle (Fig. 9). If so, one needs to envision at least partial unwinding of complementary plus and minus strands of dsRNA segments, perhaps due to extensive bending of RNA and/or RNA-protein interaction inside the Pol complex. This idea is corroborated by earlier data on partial RNase sensitivity of ϕ6 RNA genome extracted from the virions (28).

This work, as well as a number of previous studies, reports a strong effect of Mn^{2+} on RNA-dependent RNA synthesis (Fig. 5 and 6). Our previous structural studies show that Mn^{2+} binds to a specific position in the Pol subunit that is distinct from the nucleotidyltransferase site. This interaction may affect Pol polymerization efficiency, which would account for at least some of the observed effects. However, the experiments presented in

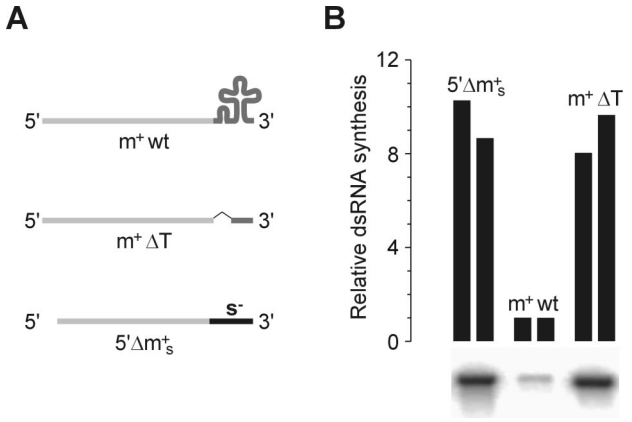

FIG. 8. The effect of ϕ6 m^+ strand 3′-proximal secondary structure in plus-strand template activity. (A) Diagram of the templates used in the experiment. m^+wt, wild-type ϕ6 m^+ segment (T7 transcript from pLM656 cut with *Xba*I and treated with mung bean nuclease [23]); $m^+\Delta T$, m^+ segment with deleted cloverleaf structure (T7 transcript from pHY3 cut with *Bpi*I); $5'\Delta m^+_s$, m^+ segment with 3′ terminal part from ϕ6 s^- (T7 transcript from pEM23 cut with *Bpu*AI [16]). (B) The RNAs were incubated with ϕ6 Pol for 1 h at 30°C as described under Materials and Methods. Reaction products were separated by standard agarose gel electrophoresis and analyzed by phosphorimaging. The autoradiogram shows bands of dsRNA synthesized in each of the three reactions. The graph on the top shows the quantification of the phosphorimager data from two independent experiments.

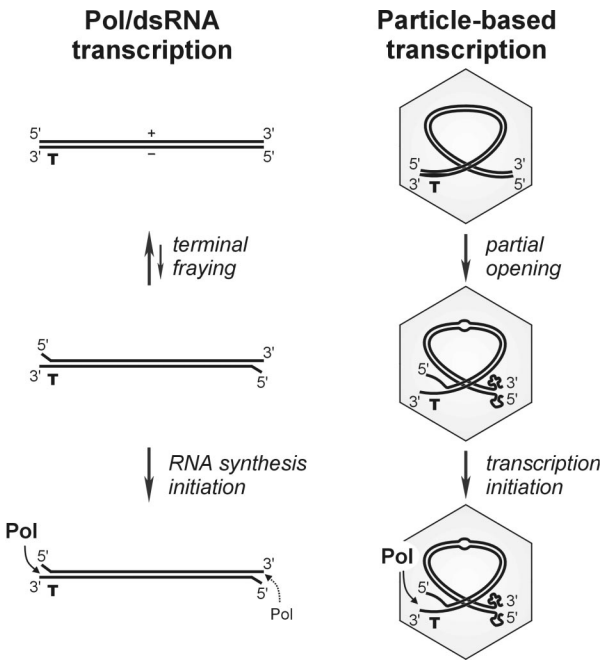

FIG. 9. Working model for transcriptional polarity in *Cystoviridae*. Production of plus-sense RNA transcripts is favored in both Pol/dsRNA and particle-based transcription systems due to at least two independent factors: Pol specificity for the 3′ terminus and the availability of the terminus in a single-stranded initiation-competent form. The latter can be controlled either through more-efficient fraying of transcription initiation end of dsRNA segments (depicted for the Pol/dsRNA system) or through the presence of stable intramolecular secondary structure at the 3′ termini of plus strands and the absence of that at the 3′ termini of minus strands (shown for a partially unwound dsRNA segment within the subviral particle).

Fig. 6C to E suggest that additional levels of regulation might be involved, such as possible interaction of Mn^{2+} directly with RNA substrate, thus affecting the polarity of newly produced transcripts. We are currently performing biochemical and structural studies that will eventually shed more light on this aspect of RNA-dependent RNA Pol functioning.

In conclusion, this study describes particle- and isolated Pol subunit-based transcription systems for cystoviruses ϕ8 and ϕ13. The results of the presented experiments indicate that, in addition to the Pol subunit template preferences, the secondary structure of genomic RNAs facilitates correct transcriptional polarity in *Cystoviridae*.

ACKNOWLEDGMENTS

We thank Riitta Tarkiainen and Marja-Leena Perälä for their expert technical assistance.

This work was supported by the Academy of Finland (Finnish Centre of Excellence Program 2000-2005, grants 162993, 164298, and 178778 to S.J.B.).

REFERENCES

1. **Bamford, D. H., P. M. Ojala, M. Frilander, L. Walin, and J. K. H. Bamford.** 1995. Isolation, purification, and function of assembly intermediates and subviral particles of bacteriophages PRD1 and ϕ6, p. 455–474. *In* K. W. Adolph (ed.), Methods in molecular genetics, vol. 6. Academic Press, San Diego, Calif.
2. **Butcher, S. J., T. Dokland, P. M. Ojala, D. H. Bamford, and S. D. Fuller.** 1997. Intermediates in the assembly pathway of the double-stranded RNA virus ϕ6. EMBO J. **16:**4477–4487.
3. **Butcher, S. J., J. M. Grimes, E. V. Makeyev, D. H. Bamford, and D. I. Stuart.** 2001. A mechanism for initiating RNA-dependent RNA polymerization. Nature **410:**235–240.
4. **de Haas, F., A. O. Paatero, L. Mindich, D. H. Bamford, and S. D. Fuller.** 1999. A symmetry mismatch at the site of RNA packaging in the polymerase complex of dsRNA bacteriophage ϕ6. J. Mol. Biol. **294:**357–372.
5. **Dubochet, J., M. Adrian, J. J. Chang, J. C. Homo, J. Lepault, A. W. McDowall, and P. Schultz.** 1988. Cryo-electron microscopy of vitrified specimens. Q. Rev. Biophys. **21:**129–228.
6. **Emori, Y., H. Iba, and Y. Okada.** 1983. Transcriptional regulation of three double-stranded RNA segments of bacteriophage ϕ6 in vitro. J. Virol. **46:** 196–203.
7. **Fields, B. N., D. M. Knipe, P. M. Howley, R. M. Chanock, J. L. Melnick, T. P. Monath, and B. Roizman.** 1996. Fields virology, 3rd ed. Lippincott-Raven, Philadelphia, Pa.
8. **Gottlieb, P., S. Metzger, M. Romantschuk, J. Carton, J. Strassman, D. H. Bamford, N. Kalkkinen, and L. Mindich.** 1988. Nucleotide sequence of the middle dsRNA segment of bacteriophage ϕ6: placement of the genes of membrane-associated proteins. Virology **163:**183–190.
9. **Gottlieb, P., J. Strassman, and L. Mindich.** 1992. Protein P4 of the bacteriophage ϕ6 procapsid has a nucleoside triphosphate-binding site with associated nucleoside triphosphate phosphohydrolase activity. J. Virol. **66:**6220–6222.
10. **Hoogstraten, D., X. Qiao, Y. Sun, A. Hu, S. Onodera, and L. Mindich.** 2000. Characterization of phi8, a bacteriophage containing three double-stranded RNA genomic segments and distantly related to ϕ6. Virology **272:**218–224.
11. **Juuti, J. T., and D. H. Bamford.** 1997. Protein P7 of phage ϕ6 RNA polymerase complex, acquiring of RNA packaging activity by in vitro assembly of the purified protein onto deficient particles. J. Mol. Biol. **266:**891–900.
12. **Juuti, J. T., and D. H. Bamford.** 1995. RNA binding, packaging and polymerase activities of the different incomplete polymerase complex particles of dsRNA bacteriophage ϕ6. J. Mol. Biol. **249:**545–554.
13. **Juuti, J. T., D. H. Bamford, R. Tuma, and G. J. Thomas, Jr.** 1998. Structure and NTPase activity of the RNA-translocating protein (P4) of bacteriophage ϕ6. J. Mol. Biol. **279:**347–359.
14. **Kenney, J. M., J. Hantula, S. D. Fuller, L. Mindich, P. M. Ojala, and D. H. Bamford.** 1992. Bacteriophage ϕ6 envelope elucidated by chemical cross-linking, immunodetection, and cryoelectron microscopy. Virology **190:**635–644.
15. **Laurila, M. R., E. V. Makeyev, and D. H. Bamford.** 2002. Bacteriophage ϕ6 RNA-dependent RNA polymerase: molecular details of initiating nucleic acid synthesis without primer. J. Biol. Chem. *in press*.
16. **Makeyev, E. V., and D. H. Bamford.** 2000. The polymerase subunit of a dsRNA virus plays a central role in the regulation of viral RNA metabolism. EMBO J. **19:**6275–6284.
17. **Makeyev, E. V., and D. H. Bamford.** 2000. Replicase activity of purified recombinant protein P2 of double-stranded RNA bacteriophage ϕ6. EMBO J. **19:**124–133.
18. **McGraw, T., L. Mindich, and B. Frangione.** 1986. Nucleotide sequence of the small double-stranded RNA segment of bacteriophage ϕ6: novel mechanism of natural translational control. J. Virol. **58:**142–151.
19. **Mindich, L.** 1999. Precise packaging of the three genomic segments of the double-stranded-RNA bacteriophage ϕ6. Microbiol. Mol. Biol. Rev. **63:**149–160.
20. **Mindich, L.** 1999. Reverse genetics of dsRNA bacteriophage ϕ6. Adv. Virus. Res. **53:**341–353.
21. **Mindich, L., I. Nemhauser, P. Gottlieb, M. Romantschuk, J. Carton, S. Frucht, J. Strassman, D. H. Bamford, and N. Kalkkinen.** 1988. Nucleotide sequence of the large double-stranded RNA segment of bacteriophage ϕ6: genes specifying the viral replicase and transcriptase. J. Virol. **62:**1180–1185.
22. **Mindich, L., X. Qiao, J. Qiao, S. Onodera, M. Romantschuk, and D. Hoogstraten.** 1999. Isolation of additional bacteriophages with genomes of segmented double-stranded RNA. J. Bacteriol. **181:**4505–4508.
23. **Olkkonen, V. M., P. Gottlieb, J. Strassman, X. Y. Qiao, D. H. Bamford, and L. Mindich.** 1990. *In vitro* assembly of infectious nucleocapsids of bacteriophage f6: formation of a recombinant double-stranded RNA virus. Proc. Natl. Acad. Sci. USA **87:**9173–9177.
24. **Paatero, A. O., L. Mindich, and D. H. Bamford.** 1998. Mutational analysis of the role of nucleoside triphosphatase P4 in the assembly of the RNA polymerase complex of bacteriophage ϕ6. J. Virol. **72:**10058–10065.
25. **Pagratis, N., and H. R. Revel.** 1990. Detection of bacteriophage ϕ6 minus-strand RNA and novel mRNA isoconformers synthesized in vivo and in vitro, by strand-separating agarose gels. Virology **177:**273–280.
26. **Qiao, X., J. Qiao, S. Onodera, and L. Mindich.** 2000. Characterization of phi 13, a bacteriophage related to ϕ6 and containing three dsRNA genomic segments. Virology **275:**218–224.
27. **Sambrook, J., and D. Russell.** 2001. Molecular cloning: a laboratory manual, 3rd ed. Cold Spring Harbor Laboratory Press, Cold Spring Harbor, N.Y.
28. **Van Etten, J. L., A. K. Vidaver, R. K. Koski, and J. P. Burnett.** 1974. Base composition and hybridization studies of the three double-stranded RNA segments of bacteriophage ϕ6. J. Virol. **13:**1254–1262.
29. **Yang, H., E. V. Makeyev, and D. H. Bamford.** 2001. Comparison of polymerase subunits from double-stranded RNA bacteriophages. J. Virol. **75:** 11088–11095.